Thermo-optic Nonlinearities in MoS_2-on-silicon Microring Resonator

(Student Paper)

Yaojing Zhang, Li Tao, Dan Yi, Jian-Bin Xu, Hon Ki Tsang
The Chinese University of Hong Kong, Shatin, New Territories, Hong Kong
e-mail: hktsang@ee.cuhk.edu.hk

ABSTRACT

In this paper, we characterize the thermo-optic nonlinearities of a MoS_2-on-silicon microring resonator under different input powers. We experimentally observe an enhanced thermal-optic effect giving rise to about three times increase in resonance shift rate compared to that of a silicon microring resonator without MoS_2.

Keywords: thermo-optic nonlinearities, MoS_2, microring resonator.

1. INTRODUCTION

Atomically thin quasi two dimensional layers of molybdenum disulphide (MoS_2) have attracted much research interest in recent years because of their high Kerr nonlinearity, estimated to be about 10^{16} m^2/W [1], and their large bandgap which is increased by quantum confinement to about 1.9 eV for the MoS_2 monolayer. However, despite its large bandgap, MoS_2 is also known to absorb photons which have less than the bandgap energy because of the presence of defect states [3], and this has allowed MoS_2 to be used as saturable absorbers in mode-locked fiber lasers [2]. Silicon microring resonators have been used in optical delay lines [3], optical modulators [4], optical switches [5] and phase shifters for optical signal processing [6]. In this paper, we investigate whether the hybrid integration of a few layers of MoS_2 on a silicon microring resonator can enhance their Kerr nonlinearity or whether the optical characteristics of the microring is dominated by the defect state absorption in MoS_2 and thermal nonlinearity. We transfer the multi-layer MoS_2 onto the top of a silicon microring resonator. We measure the resonance shifts at different levels of continuous wave input optical powers coupled into the device. Our experimental results exhibit a large thermo-optic effect with a resonance shift rate of 0.24 nm/mW, which is about three times larger than that of a silicon microring but without the coverage of MoS_2.

2. FABRICATION

We fabricate the silicon resonator on the SOI wafer. The top silicon thickness is 250 nm and the buried oxide (BOX) is nominally 3 μm thick. The widths and heights of both bus waveguide and ring are designed as 500 nm and 250 nm, respectively. The width of gap between the bus waveguide and ring is designed to be 100 nm and the diameter of the ring resonator is about 40 μm as shown in the scanning electron microscopy (SEM) image of Figure 1(a). The light is coupled into the waveguide through uniform grating couplers. For the fabrication, we pattern both device and gratings with electron-beam lithography process. Then we deeply etch them with reactive-ion etching process. Multi-layer MoS_2 film (thickness ~5 nm) is grown on SiO_2/Si substrate by chemical vapor deposition, of which the details can be found in our previous paper [7]. Afterwards, the MoS_2 film is transferred onto the target ring resonator through a dry method assisted by viscoelastic polyvinyl alcohol film [8]. The length of the coverage is about 47 μm.

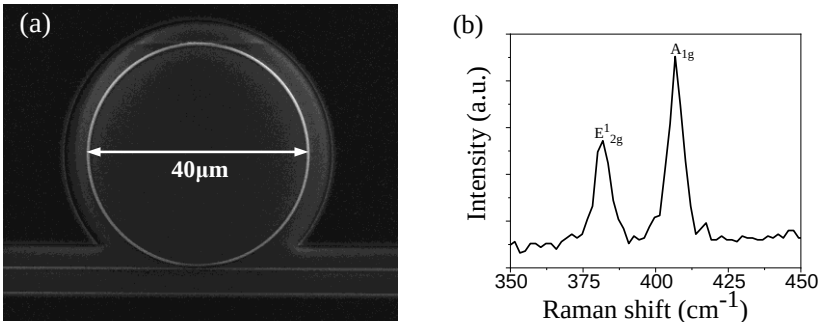

Figure 1. (a) SEM image of silicon ring resonator. (b) Raman spectrum of MoS_2 film used as the coverage of silicon ring resonator.

3. EXPERIMENTAL RESULTS AND ANALYSIS

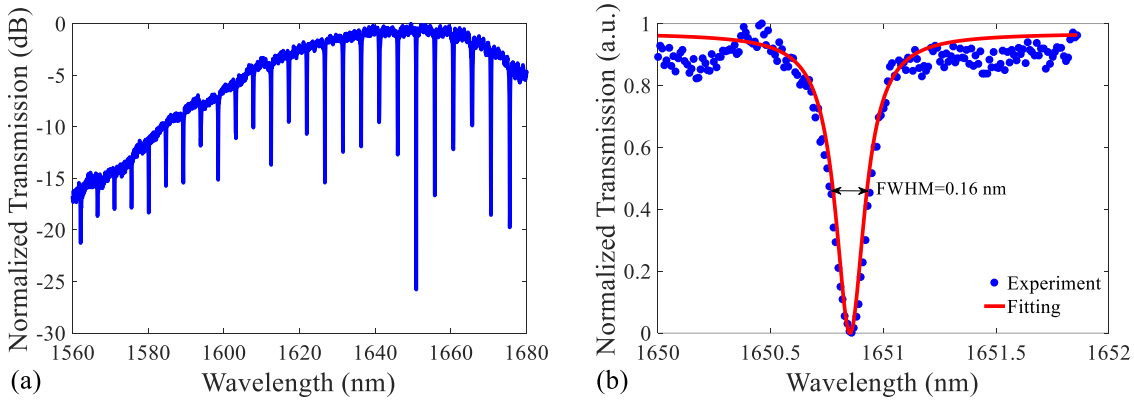

Figure 2. (a) Normalized transmission as a function of input wavelength with range from 1560 to 1680 nm. (b) Normalized transmission around 1651 nm with fitting curve from which its FWHM can be obtained as about 0.16 nm.

We first characterize the transmission of the resonator at a low coupled power. The quasi TM polarized light generated from a continuous-wave laser with power of 0.1 mW is the incident power at the waveguide grating coupler. We obtain the total fiber-chip-fiber insertion loss is about 20 dB. The free spectral range (FSR) of the microring is about 4.9 nm around 1651 nm as shown in Figure 2(a). The measured full width at half maximum (FWHM) of the resonance around 1651 nm is measured to be about 0.16 nm as shown in Figure 2(b) and the loaded quality factor derived from this measurement is $Q_L = \lambda_0/FWHM$=10300 (λ_0 is the resonant wavelength under low input power). The intrinsic quality factor $Q_i = 2Q_L/(1+\sqrt{T_0})$ (T_0 is the normalized transmission at resonant wavelength shown in Figure 2) [9] is estimated to be 19800 and the loss of ring per roundtrip is $\alpha_r = \lambda_0/(FSR \cdot Q_i \cdot R) = 8.5\ cm^{-1}$ (R is the radius of the ring) [9].

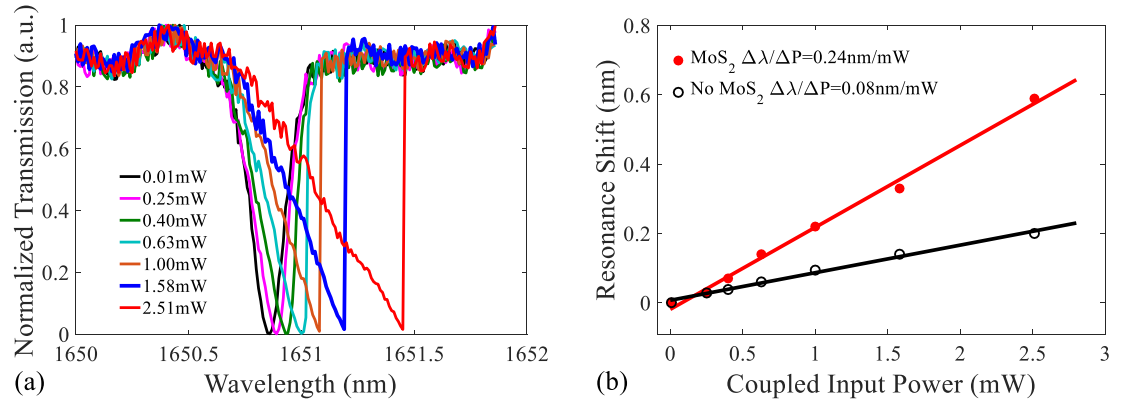

Figure 3. (a) Experimental transmission spectra at different coupled input power levels for MoS_2-on-silicon ring resonator which shows obvious thermal nonlinearities when we increase the input power. (b) Resonance shift versus coupled input power in the measurement and its corresponding fitting curve.

Next, with the same experimental setup, we increase the coupled input power into the waveguide and record the corresponding transmission around resonant wavelength of 1651 nm as shown in Figure 3(a). The coupled input power is after the loss of one grating coupler. At a low power, the resonant shape is symmetric while its shape becomes asymmetric and broader with the increase of power. The resonant wavelength is red-shifted with the increased input power. With the enhancement of the input power, thermo-optic effect leads to the redshifted resonant wavelength unlike free-carrier dispersion effect which would produce a blue shift [10]. Both phenomena stem from the changes of refractive index. In our case, the resonant wavelength is clearly redshifted with the increasing input power suggesting that the thermo-optic effect is the dominant mechanism for the nonlinear shift in resonant wavelength. Figure 3(b) illustrates the relation between the coupled input power and resonance shift and the resonance shift rate is obtained as about 0.24 nm/mW for MoS_2-on-silicon resonator while that of bare silicon resonator is 0.08 nm/mW. In the MoS_2-on-silicon resonator, the MoS_2 film absorbs the light owing to its defect states and further converts it to heat, leading to a various effective index of the waveguide due to the thermo-optic effect [11,12]. The varied effective index induces the resonance shift of the resonator.

4. CONCLUSIONS

We experimentally investigate thermal nonlinearities in MoS_2-on-silicon microring resonator. The corresponding loaded quality factor due to the additional loss from MoS_2 film is obtained as 10300. However, we observe three times increase in resonance shift rate compared to that of device without MoS_2 for the additional absorption of light from MoS_2 film due to its defect states and further converting it to heat.

ACKNOWLEDGEMENTS

This work was fully funded by Hong Kong Research Grant Council (RGC) GRF Project No. 14203318.

REFERENCES

[1] L. Liu, *et al.*: Enhanced optical Kerr nonlinearity of MoS_2 on silicon waveguides, *Photonics Res.*, vol. 3. pp. 206-209, Oct. 2015.

[2] M. Liu, *et al.*: Microfiber-based few-layer MoS_2 saturable absorber for 2.5 GHz passively harmonic mode-locked fiber laser, *Opt. Express*, vol. 22. pp. 22841-22846, Sep. 2014.

[3] J. Cardenas, *et al.*: Wide-bandwidth continuously tunable optical delay line using silicon microring resonators, *Opt. Express*, vol. 18. pp. 26525-26534, Dec. 2010.

[4] Q. Xu, *et al.*: 12.5 Gbit/s carrier-injection-based silicon micro-ring silicon modulators, *Opt. Express*, vol. 15. pp. 430-436, Jan. 2007.

[5] V. R. Almeida, *et al.*: All-optical switching on a silicon chip, *Opt. Lett.*, vol. 29. pp. 2867-2869, Dec. 2004.

[6] Q. Chang, *et al.*: A tunable broadband photonic RF phase shifter based on a silicon microring resonator, *IEEE Photonic. Tech. L.*, vol. 21. pp. 60-62, Jan. 2009.

[7] L. Tao, *et al.*: Centimeter-scale CVD growth of highly crystalline single-layer MoS_2 film with spatial homogeneity and the visualization of grain boundaries, *ACS Appl. Mater. Interfaces*, vol. 9. pp. 12073-12081, Mar. 2017.

[8] L. Tao, *et al.*: Deterministic and Etching-Free Transfer of Large-Scale 2D Layered Materials for Constructing Interlayer Coupled van der Waals Heterostructures, *Adv. Mater. Technol.*, vol. 3. pp. 1700282, May 2018.

[9] L.-W. Luo, *et al.*: High quality factor etchless silicon photonic ring resonators, *Opt. Express*, vol. 19. pp. 6284-6289, Mar. 2011.

[10] L. Zhang, *et al.*: Experimental observations of thermo-optical bistability and self-pulsation in silicon microring resonators, *JOSA B*, vol. 31. pp. 201-206, Feb. 2014.

[11] C. Horvath, *et al.*: Photothermal nonlinearity and optical bistability in a graphene-silicon waveguide resonator, *Opt. Lett.*, vol. 38. pp. 5036-5039, Dec. 2013.

[12] T. Gu, *et al.*: Molecular-absorption-induced thermal bistability in PECVD silicon nitride microring resonators, *Opt. Express*, vol. 22. pp. 18412-18420, Jul. 2014.